Enabling Better Thermal Management of Indoor Spaces through Adaptive Zonal Heat Transfer

Zaid Bin Tariq, Koushik Kar, Sandipan Mishra, John T. Wen
Rensselaer Polytechnic Institute
110 8th Street, Troy, NY 12180.
Email: {tariqz, kark, mishrs2, wenj}@rpi.edu

***Abstract*—In multi-zone indoor spaces with thermal dependencies between zones and limited heating/cooling sources, choosing optimal zonal thermostat or heat input settings is often not enough to attain desired zonal temperatures. In such scenarios, simple changes that affect the thermal transfer between different zones, or between the individual zones and the ambient – actuated through opening/closing of doors and windows, for example – can significantly improve the the zonal temperatures or reduce energy costs. In this paper, we consider the problem of determining how the thermal flow in-between the different zones of the indoor space, or between the zones and the ambient, should be adapted towards improving the overall thermal environment in the multi-zone space. Despite the complex structure of the problem, we show how such the question of optimal zonal heat transfer adaptation – which involves determining the optimal zonal heat input settings as well – can be formulated and solved efficiently. We also determine conditions under which the problem has a convex structure. Finally, we evaluate the benefits of zonal heat transfer adaptation through simulations on a dynamic thermal model of a 6-zone indoor space. Our results show that zonal heat transfer adaptation can result in significant improvement of zonal temperatures and/or energy costs, particularly when not all zones are equipped with heat sources.**

I. Introduction

Improving occupant comfort in an indoor environment is typically associated with increased energy cost. Therefore, attaining the optimal thermal environment in indoor spaces would require modeling and optimizing the trade-off between the comfort and energy costs. Attaining this balance in multi-occupant multi-zone spaces (such as shared office and dorm spaces, and even residential buildings), is challenging due to several reasons. Firstly, the desired temperature preferences of the occupants of the indoor space are often in conflict with each other. Secondly, there are complex thermal dependencies between the different "zones" of the space, due to the natural flow of heat (air) between adjacent zones. Thirdly, some zones may not be equipped with heating/cooling sources, and therefore their thermal environment may not be controllable via direct means. Due to the last two reasons, even if the occupants occupy different zones in the indoor space, it may not be possible for the building thermal management system (BTMS) to attain the occupants' desired temperatures in their respective zones.

In the literature, a variety of methods have been proposed towards improving occupant comfort. For example, a model predictive method using surface level weather forecasts and multi-tiered implementation strategy is proposed in [1]. A HVAC control framework that integrates environmental data with the human physiological and behavioral data obtained using different wearable devices is proposed in [2]. The authors in [3] use model predictive control with a zone operative temperature comfort metric that accounts for radiative impacts on comfort. The authors in [4] consider the estimation of distributed parameters of a multi-room building towards maximizing observability and controllability. Our prior work on indoor thermal environment control [5], [6], [7] have focused on optimizing the trade-off between aggregate user discomfort and total energy usage in the building. While the optimization problem in that case has a convex structure, the goal of these prior work has been the design of incentive mechanisms and distributed control algorithms to a) elicit truthful comfort preference feedback from the occupants, b) attain a thermal consensus between occupants of the shared space, and c) converge to the optimal zonal temperatures under the thermal dynamics of the space. These prior solutions optimize the BTMS operations (through the zonal thermostat settings or heat inputs) for the indoor space, when the heat transfer settings between the different zones, and between the zones and the ambient, are assumed to be given (unchangeable).

In this paper, we recognize that there is often some flexibility associated with these zonal heat transfer (ZHT) settings - which can be attained by simply opening the doors or windows associated with the zones, or controlling the direction or speed of fans installed for air/heat exchange between zones - and aim to utilize it for attaining better zonal temperatures and reducing energy cost. In fact, in certain scenarios the desired zonal temperatures may not even be attainable without ZHT adaptation (i.e., with thermostat/heat input control alone). This is often the case when the number of control elements (heat inputs or thermostat controls) is less than the number of thermal zones. In other scenarios, where the desired zonal temperatures is attainable through thermostat/heat input control, ZHT adaptation could help in reducing energy usage.

We make the following contributions in this paper. Firstly, we formulate the problem zonal heat transfer (ZHT) adaptation as a non-linear optimization question under steady state conditions of the thermal dynamics, derived on the basis of a RC thermal model of the system. We then utilize some structural properties of the model to show how the complexity of finding the optimal solution can be reduced significantly. Towards that end, we first show that the problem of joint determination of optimal ZHT settings and heat input vector is equivalent to a reduced-order problem of only determining the ZHT settings optimally. Secondly, we show that under a limiting condition of the parameter that dictates the trade-off between energy cost and thermal discomfort, our optimization objective has a convex structure that allows solution using standard convex optimization techniques. Thirdly, we show how the dimensionality and complexity of the model/problem further reduces in a "thin wall" scenario, and when all zones are equipped with heat sources. Finally, we demonstrate the benefits of using ZHT adaptation – in terms of zonal temperature deviations from desired settings, and total energy usage – on a realistic 6-zone indoor space model based on our test facility in Watervliet, NY.

II. Model and Formulation

A. Electrical Analogy based Heat Transfer model

Before formulating the problem of optimal ZHT adaptation, we describe the heat transfer model that we use in our study. In the literature, multiple strategies have been proposed to model the thermal dynamics of a building. These include finite element method based model [8], lumped mass and energy transfer model [9] and models based on the electric circuit analogy of a thermal system [10], [11]. In this paper, we will utilize this thermal model based on electrical circuit analogy, which we found to be quite effective in modeling and analyzing related problems in our prior work [6], [5], [12]. In this model, each room acts as a thermal capacitor and the walls form an RC network. The zones in a system are interconnected with the resistances to form a lump heat transfer model. This results in the standard lumped 3R2C wall model [11]. The heat flow modeling is based on temperature difference and thermal resistance: $Q = \Delta T/R$, where ΔT is the temperature difference, R is the thermal resistance and Q is the heat transferred across the resistance.

In this model, let the temperature of a i^{th} capacitor be T_i and let there be n thermal capacitors interconnected by l thermal resistors. Let T_∞ be a scalar representing the ambient temperature. Then the heat transfer model of a system with m zones, of which k ($\leq m$) zones are equipped with heat sources, is given by [13]:

$$C\dot{T} = -DR^{-1}D^T T - DR^{-1}d_o^T T_\infty + \tilde{B}u, \quad (1)$$

where $T \in \mathbb{R}^n$ is the temperature vector of the thermal capacitors in the 3R2C model (which includes the rooms/zones as well), $u \in R^k$ is the vector of heat inputs into the different zones of the space, and $\tilde{B}$ is the corresponding $n \times k$ input matrix with only 0 and 1 elements. In the above equation, $C \in \mathbb{R}^{n\times n}$ consists of the zone and wall capacitances and is a diagonal positive definite matrix; $R \in \mathbb{R}^{l\times l}$ consists of the thermal resistors in the system and is a diagonal positive definite matrix as well. Also, $D \in \mathbb{R}^{n\times l}$ is the incidence matrix, mapping the system capacitances to the resistors, and is of full row rank [14], and $-DR^{-1}d_0^T \in \mathbb{R}^n$ is a column vector with non-zero elements denoting the thermal conductances of nodes connected to the ambient. Also, note that (T,u) are functions of time $(T(t),u(t))$ and accordingly $\dot{T} = \frac{dT}{dt}$. Note that positive values of u correspond to heating the system while negative values of u correspond to cooling. The vector of zone temperatures, denoted by y (which is a function of T) can be expressed as

$$y = B^T T, \quad (2)$$

where B is an $m \times n$ matrix with only 0 and 1 elements. While multiple heat inputs in a any zone can be clubbed together into a single heat input for that zone, some zones may not have any heat inputs. Therefore, $\tilde{B}$ may be "smaller than" B, i.e., $k \leq m$. Apart from this difference, our model is the same as that used in our prior work [6], [5], [12]. In practice, it is typical for only some of the zones to be equipped with heat inputs (heating/cooling units). This is also the scenario ($k < m$) where zonal heat transfer adaptation can make a major difference in the zonal temperatures attained and/or the total energy consumed, as we will see later.

B. Optimization Objective

The zonal heat transfers can be adapted only by adjusting the thermal resistances in R in (1). For ease of exposition and analysis, we represent (1) in terms of the conductance matrix $\Theta = R^{-1}$. Note that each element in Θ is simply the conductance (inverse of the resistance) of the corresponding resistive element of R. Since we pose the optimization objective under steady state conditions, setting $\dot{T} = 0$ in (1) yields $T = (-D\Theta D^T)^{-1}(D\Theta d_o^T T_\infty + \tilde{B}u)$. Defining matrix $A = (D\Theta D^T)^{-1}$, and vector $\Lambda_\infty = -D\Theta d_o^T$, we have the following steady state condition:

$$T = A^{-1}(\Lambda_\infty T_\infty + \tilde{B}u). \quad (3)$$

Note that in general Θ includes conductances associated with the internal as well as the external walls. Some of these conductances may not be adjustable, e.g., fixed walls with no doors of windows in them. In general, opening (closing) of a door or window results in a increase (decrease) of the conductance associated with that wall. Further, all doors and windows may not be opened or closed due to privacy or security reasons, or simply occupant preference. Let θ be the vector of all conductances in the system, and $\underline{\theta}$ represents the set over which θ is constrained to vary. We assume that $\underline{\theta}$ is in the form of box constraints, $[\theta_{\min}, \theta_{\max}]$. Note that this $[\theta_{\min}, \theta_{\max}]$ range depends on the maximum and minimum open/close settings of the doors and windows; if the resistance (conductance) of a particular element (wall) cannot be adapted, then for that particular element i, $\theta_{\min,i} = \theta_{\max,i}$. We assume that the vectors $\theta_{\min}, \theta_{\max}$ can be learned by the thermal management system through a model estimation process – based on zonal temperature measurements collected over time – as in our prior work [12].

We assume that each of the m zones has a desired temperature (possibly determined based on the occupants' preferences). Let $\hat{y}$ denote that desired zonal temperature vector. Let $\hat{\theta}$ be a desired conductance level, which may correspond to a preferred setting of the controllable doors and windows. Then our optimization objective is defined as

$$\begin{aligned} \min_{y,u,\theta} \quad & ||y-\hat{y}||^2+\alpha||u||^2+\beta||\theta-\hat{\theta}||^2 \\ \text{s.t.} \quad & (2),(3), \text{ and } \theta \in \underline{\theta}. \end{aligned} \tag{4}$$

III. Analysis

The problem posed in (4) is a complex optimization question. In this section, we will provide methods that can reduce the complexity of solving the problem, so that it can be solved exactly in reasonable computation time. Since $\hat{y}$ may be calculated based on the preferences of the occupants occupying each zone [6], this problem may need to be re-solved every time there is a change in user occupancy in any zone. Part of the complexity of the problem is due to its dependence on three sets of variables (vectors) T,u,θ. We will progressively reduce this problem to one that only involves θ, and then study the structural properties of the reduced problem. Our first step to reducing complexity is to use (2) and (3) to replace y (as a function of u,θ) in (4). With this, and recognizing the dependence of matrix A and vector Γ_∞ on θ, we can re-express the our optimization objective in (4) as

$$\begin{aligned} \min_{u,\theta} J(u,\theta) \;=\; & ||B^TA^{-1}(\theta)(\Lambda_\infty(\theta)T_\infty+\tilde{B}u)-\hat{y}||^2 \\ & +\alpha||u||^2+\beta||\theta-\hat{\theta}||^2 \\ \text{s.t.} \quad & \theta \in \underline{\theta}. \end{aligned} \tag{5}$$

It is worth noting that if the zonal heat transfer parameters are all assumed given, then A and Λ_∞ are constant, and (5) involves only optimization over u, which is a quadratic programming problem and can be solved efficiently. In general, however, $A(\theta)=-D\Theta(\theta)D^T$, and vector $\Lambda_\infty(\theta)=-D\Theta(\theta)d_o^T$, are functions of θ. Note that while $A(\theta)$ and $\Lambda_\infty(\theta)$ are linear functions of θ, $A^{-1}(\theta)$ that appears in the objective $J(u,\theta)$ can be a complex function of θ.

The next step in reducing our optimization problem to a simpler form is to express the optimal u in (5) as a function of θ, $u^*(\theta)$. Let $g(\theta)=\min_u J(u,\theta)=J(u^*(\theta),\theta)$. Clearly, our optimization problem in (5), $\min_{u,\theta} J(u,\theta)$, can be expressed as $\min_{\theta\in[\theta_{\min},\theta_{\max}]} g(\theta)$. Optimizing $J(u,\theta)$ over u for a given θ results in

$$\begin{aligned} u^* \;=\; & (\alpha I_k+P^TP)^{-1}P^T(\hat{y}-B^TA^{-1}\Lambda_\infty T_\infty), \\ & \text{where} \quad P=B^TA^{-1}\tilde{B}, \end{aligned} \tag{6}$$

and I_k is an $k\times k$ identity matrix. The dependency of u^* on θ is realized be recognizing that P,A and Λ_∞ are all functions of θ.

Plugging u^* from (6) in the objective function of (5), following some algebraic manipulation, we obtain $g(\theta)$ as

$$\begin{aligned} g(\theta) \;=\; & \alpha Z^T(\theta)(\alpha(P^T(\theta)P(\theta))^{-1}+I_k)^{-1}Z(\theta) \\ & +\beta||\theta-\hat{\theta}||^2, \\ & \text{where} \quad Z(\theta)=P^+(\theta)(\hat{y}-B^TA^{-1}(\theta)\Lambda_\infty(\theta)T_\infty), \end{aligned} \tag{7}$$

and P^+ is the pseudo-inverse of the $m\times k$ matrix $P=B^TA^{-1}\tilde{B}$, which has a full rank $k\le m$. Note that $P^+P=I_k$. Further note that P^TP is positive definite, and the terms $(\alpha I_k+P^TP)^{-1}$ in (6) and $(\alpha(P^TP)^{-1}+I_k)^{-1}$ in (7) exist.

Defining $Q=(\alpha(P^TP)^{-1}+I_k)^{-1}$, $g(\theta)$ is expressed as $g(\theta)=\alpha Z^T(\theta)Q(\theta)Z(\theta)+\beta||\theta-\hat{\theta}||^2$. Note that for "small" α, $Q(\theta)$ approaches 1, and therefore $g(\theta)$ approaches $\alpha Z^T(\theta)Z(\theta)+\beta||\theta-\hat{\theta}||^2$, a quadratic form in $Z(\theta)$, plus a quadratic term in θ. However, note that $Z(\theta)$ can potentially be a complex function of θ. We however show below that for "sufficiently small" α, $g(\theta)$ is convex.

Define $f(\theta)=Z^T(\theta)Q(\theta)Z(\theta)=Z^T(\theta)(\alpha(P^T(\theta)P(\theta))^{-1}+I_k)^{-1}Z(\theta)$. It can be shown that $||\nabla^2 f(\theta)||$, the L_2-norm of the Hessian of the function $f(\theta)$, is bounded for all $\theta\in\underline{\theta}=[\theta_{\min},\theta_{\max}]$, under the reasonable assumption that $\theta_{\min}>0$, i.e., the capacitance values of all resistors in our model are bounded away from zero. Let L be an upper bound on this norm, i.e., $L=\max_{\theta\in\underline{\theta}}||\nabla^2 f(\theta)||$.

Proposition III.1. *For all α satisfying $0<\alpha<\frac{2\beta}{L}$, $g(\theta)$ as expressed in (7) is strictly convex in θ, and the optimization problem $\min_{\theta\in\underline{\theta}} g(\theta)$ has a unique optimizer θ^*.*

Proof. To show that $g(\theta)$ is strictly convex in $\theta\in\underline{\theta}$, it suffices to show that $\nabla^2 g(\theta)$ is positive definite for all $\theta\in\underline{\theta}$. If we define $h(\theta)=||\theta-\hat{\theta}||^2$, we have $\nabla^2 g(\theta)=\alpha\nabla^2 f(\theta)+\beta\nabla^2 h(\theta)=\alpha\nabla^2 f(\theta)+2\beta I_l$. Since $\nabla^2 f(\theta)$ and I_l are both Hermitian, from Weyl's theorem it follows that for any given θ, $\lambda_{\min}(\nabla^2 g)$ and $\lambda_{\min}(\nabla^2 f)$, the minimum eigenvalues of $\nabla^2 g(\theta)$ and $\nabla^2 f(\theta)$, respectively, are related by

$$\lambda_{\min}(\nabla^2 g)=\alpha\lambda_{\min}(\nabla^2 f)+2\beta. \tag{8}$$

Next we argue that $\lambda_{\min}(\nabla^2 f)$ (which depends of θ, since f is a function of θ) is lower-bounded (i.e., can not be arbitrarily negative) for any $\theta\in\underline{\theta}=[\theta_{\min},\theta_{\max}]$, when $\theta_{\min}>0$. Towards that end, we first argue that $||\nabla^2 f(\theta)||$ is upper bounded. Recall that $f(\theta)=Z^T(\theta)Q(\theta)Z(\theta)=Z^T(\theta)(\alpha(P^T(\theta)P(\theta))^{-1}+I_k)^{-1}Z(\theta)$, where $Z(\theta)$ is defined as in (7), $P(\theta)$ is given by (6), and P^+ the pseudo-inverse of P, is obtained as $P^+=(P^TP)^{-1}P^T$. The derivation of $\nabla^2 f(\theta)$ is fairly tedious, and the final expression is quite complex. From the definition of $P(\theta),Z(\theta)$, and the fact that $\Gamma_\infty(\theta)=-DA(\theta)d_0^T$, we note however that $f(\theta)$ depends on θ only through the matrices $A(\theta)$,$A^{-1}(\theta)$. Assuming $\theta_{\min}>0$ (and obviously $\theta_{\max}<\infty$), the matrix $A(\theta)$ is positive definite and symmetric, and therefore has positive (and bounded) eigenvalues $\mu_i, i=1,\cdots n$, The eigenvalues of the matrix $A^{-1}(\theta)$ are then $\frac{1}{\mu_i}, i=1,\cdots,n$, which are therefore positive and bounded as well. Therefore, $||A(\theta)||$ and $||A^{-1}(\theta)||$ are bounded for all $\theta\in\underline{\theta}$. Note further that since $A=-D\Theta D^T$, for any two components θ_i,θ_j of θ, $\frac{\partial A}{\partial\theta_i}$ is a constant matrix, and $\frac{\partial^2 A}{\partial\theta_i\partial\theta_j}=0$. Further note that $\frac{\partial A^{-1}}{\partial\theta_i}=-A^{-1}\frac{\partial A}{\partial\theta_i}A^{-1}$. These imply that all elements of the Hessian $\nabla^2 f(\theta)$ can be expressed in terms of $A(\theta)$,$A^{-1}(\theta)$ and constant matrices. Since $||A(\theta)||$ and $||A^{-1}(\theta)||$ are bounded (since they have bounded eigenvalues) for all $\theta\in\underline{\theta}$, it follows that $||\nabla^2 f(\theta)||$ is upper bounded for all $\theta\in\underline{\theta}$, i.e., $L=\max_{\theta\in\underline{\theta}}||\nabla^2 f(\theta)||$ is finite. This implies that $|\lambda_{\min}(\nabla^2 f)|\le L$, which implies $\lambda_{\min}(\nabla^2 f)\ge -L$ for all $\theta\in\underline{\theta}$.

Using $\lambda_{\min}(\nabla^2 f)\ge -L$ in (8), we get $\lambda_{\min}(\nabla^2 g)\ge -\alpha L+2\beta$, which is strictly positive when $\alpha<\frac{2\beta}{L}$. This implies that all eigenvalues of $\nabla^2 g$ are positive, and hence $\nabla^2 g(\theta)$ is positive definite, for all $\theta \in \underline{\theta}$. $\square$

Note that when $g(\theta)$ is convex, the optimum zonal heat transfer setting θ^* that attains the minimum in $\min_{\theta \in \underline{\theta}} g(\theta)$ can be computed efficiently by standard convex optimization methods. While the bound $\frac{2\beta}{L}$ required for strict convexity of $g(\theta)$ (as stated in Proposition III.1) is typically very conservative, our experiments suggest that standard optimization solvers converge quickly and yield good solutions for the problem $\min_{\theta \in \underline{\theta}} g(\theta)$ for a wide range of α. It is noteworthy however, that the best relative performance of zonal heat transfer adaptation (over no zonal heat transfer adaptation) occurs when α is relatively small (as we will see in Section IV), which is what one might want to use in practice. Since $g(\theta)$ is strictly convex for small values of α, our optimization problem should be efficiently solvable in this useful range of α.

We conclude this section by identifying some practical scenarios and assumptions under which the computation of θ^*, u^* is further simplified. In the 3R2C model (which considers capacitances associated with all walls), the number of capacitance elements in the model (n) can be quite large. Under a "thin wall" assumption, which assumes walls have negligible heat retaining capacity, only the zones contribute to capacitors in the model. Thus $n = m$, and therefore $T = y$, which reduces the complexity of the model quite significantly. As an example, for the 6-zone building model shown in Figure 1 (which will be used in our simulation based evaluation is Section IV), under this "thin wall" our model comprises of 6 capacitors (one for each zone $1, \cdots, 6$) and 14 resistors (one from each of the zones to the outside, and one across each wall between adjacent zones). Since $B = I_m = I_n$ (an identity matrix) in this case, $P = B^T A^{-1} \tilde{B} = A^{-1} \tilde{B}$ in the expressions and analysis provided earlier.

Additionally, if each zone is equipped with a heat input, then $k = m$. In this case, $\tilde{B} = I_k = I_m = I_n$. Further, $P = A^{-1}$, and $P^+ = A$. Therefore, $Z(\theta) = (A(\theta)\hat{y} - \Lambda_\infty(\theta) T_\infty)$. Since both $A(\theta)$ and $\Lambda_\infty(\theta)$ are linear in θ, $Z(\theta)$ is linear in θ as well. In this special case, $g(\theta)$ reduces to

$$g(\theta) = \alpha \, (A(\theta)\hat{y} - \Lambda_\infty(\theta) T_\infty)^T \times (\alpha A^{-2}(\theta) + I)^{-1} \times (A(\theta)\hat{y} - \Lambda_\infty(\theta) T_\infty). \quad (9)$$

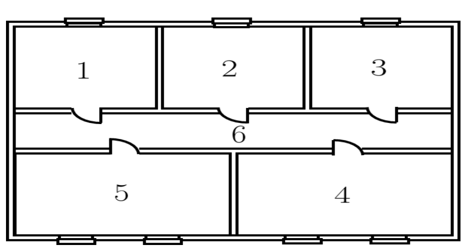

Figure 1: Layout of our test facility in Watervliet, NY, that consists of 6 zones. Zones 1-5 are rooms with windows to the outside (ambient), and doors to the central corridor. The central corridor (zone 6) has a door to the outside. Our experiments were run on an RC thermal model of this test facility, where the model parameters were learned (estimated) from temperature measurements from the different zones.

IV. Performance Evaluation

In this section, we demonstrate the benefits of adapting the zonal heat transfer (ZHT) settings through experimental evaluation in the multi-zone indoor space model described in Figure 1. The details of the the testbed facility and the corresponding RC model can be found in [15]. Briefly, the testbed consists of 6 zones with in a larger enclosure (which simulates ambient around the indoor system). The enclosure has heating sources to simulate the ambient temperature T_∞. Rooms 1 to 5 (zones 1 to 5) have a dedicated heating source, along with doors to the central corridor (zone 6) and windows to the ambient. The central corridor (zone 6) also has a door opening to the ambient. Multiple temperature sensors are placed with in each zone. We conducted experiments on a model of this system under various configurations of the heat input elements: from a case where all zones have heat input elements in them to scenarios where only a few of them zones can be heated/cooled directly. ZHT adaptation improved our system objective (as described in (4)) in all cases. ZHT adaptation was observed to be particularly beneficial when one or more zones do not have a heating source. This is not surprising: when some of the zones are not attached to a heat source, they can only be heated/cooled indirectly (by heat flows from other zones and/or from the ambient) by opening the the doors and/or windows, chosen appropriately. Our formulation and solution, as described earlier in the paper, helps determine which doors and windows should be opened in all these cases to make the ZHT adaptation most effective.

In the experimental results shown below, the desired zonal temperature vector $\hat{y}$ is chosen as follows: $\hat{y} = [70, 70, 65, 70, 70, 65]$. We present the results for two scenarios. In scenario 1, only zone 6 does not have an attached heat input source. In scenario 2, in addition to zone 6, zone 5 also does not have an attached heat input source. Since we consider cooling to be negative heat input, a heat input source can provide both heating and cooling to the zone it is attached to. We work with an RC thermal of the system under a "thin wall" assumption which ignores all wall capacitances, i.e., only considers capacitances for the 6 zones in the model. This is a reasonable assumption for our testbed (and in many scenarios in practice) and greatly reduces model complexity. In the results shown below, the ambient temperature $T_\infty = 80F$ which is used simulate mildly warm conditions and is assumed to be constant. The limits of the conductance values associated with the opening/closing of doors and windows were estimated by analyzing the data collected from the experimental testbed under fully open and closed door/window configurations.

For the case of no ZHT adaptation, the optimal heat input vector u^* can be calculated directly from (6) for a given θ (default setting). The default setting corresponds to the scenario where all doors and windows are closed, resulting in minimal heat transfer between the different zones, and between the zones and the ambient. For the case with ZHT adaptation, the optimal ZHT values (conductances) are calculated by optimizing $g(\theta)$ expressed in (7) subject to the limits

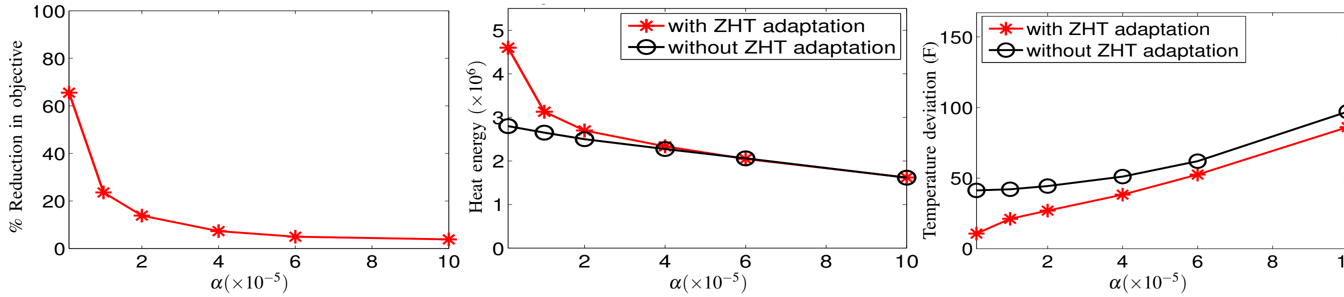

(a) % Reduction in objective (b) Heat energy (c) Temperature deviation

Figure 2: Scenario 1 (Only zone 6 does not have a heat source): Plot of the (a) total objective in (4), (b) heat energy $||u||^2$ and (c) temperature deviation $||y-\hat{y}||^2$ against α, with and without ZHT adaptation.

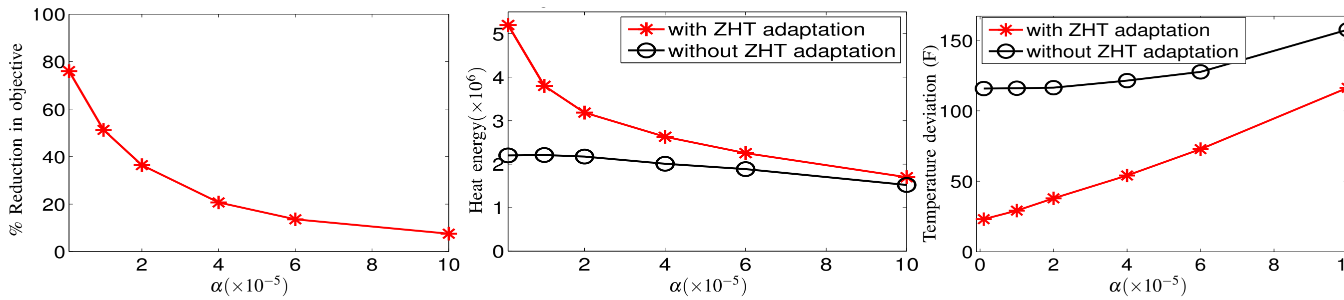

(a) % Reduction in objective (b) Heat energy (c) Temperature deviation

Figure 3: Scenario 2 (Zones 5 and 6 do not have a heat source): Plot of the (a) total objective in (4), (b) heat energy $||u||^2$ and (c) temperature deviation $||y-\hat{y}||^2$ against α, with and without ZHT adaptation.

$[\theta_{\min}, \theta_{\max}]$ using MATLAB. Once the optimum conductance value (θ^*) has been computed, the corresponding optimal heat input vector (u^*) is calculated directly from (6) for that θ^*. The dynamic response of the system is them simulated using the system dynamics described in (1)-(2) to confirm whether the actual zonal temperatures reach values predicted by our steady-state analysis.

Note that the value of α signifies the relative importance given to the energy usage vs the temperature deviation from the desired values. Since from (2), (3), we have $y \sim B^T A^{-1} \tilde{B} u$, it is easy to see that to make the temperature deviation (occupant discomfort) cost $||y-\hat{y}||^2$ and energy cost $||u||^2$ of the same order, $\alpha \sim ||A^{-2}||$. For the values over which the matrix $A(\theta)$ varies in our experiments, the range of $\alpha \sim 10^{-6}$ to 10^{-4}. For teh results shown below, therefore, α is varied over this range. Also note that for the purpose of comparison, we have used a very small value of β so that the solution of (4) is not affected by the term $\beta||\theta-\hat{\theta}||^2$.

For scenario 1 (only zone 6 is not equipped with a heat source), Figure 2a shows the improvement in the total objective function due to the use of ZHT adaptation, for different values of α. The total objective corresponds to $||y-\hat{y}||^2 + \alpha||u||^2$ since the $\beta||\theta-\hat{\theta}||^2$ term in (4) in negligible in our case. The percentage improvement in the objective function due to ZHT adaptation is approximately 66% for smaller values of α. This difference decreases with α but is always positive, as expected. From Figure 2b, we observe that the amount of energy used by the two cases (with and without ZHT adaptation) is approximately same, except when α is very small. However, the impact on the temperature deviation (Figure 2c) is quite significant: the

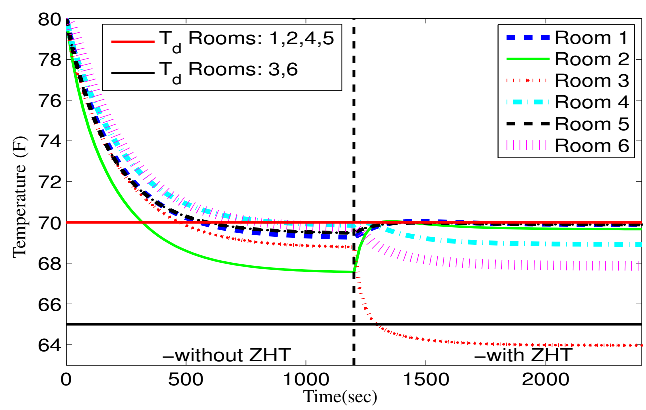

Figure 4: Zonal temperature dynamics under scenario 1 (only zone 6 does not have a heat source), with ZHT method being used from 1200 secs with the corresponding zonal temperature getting nearer to the desired temperature vector $T_d = [70, 70, 65, 70, 70, 65]$

deviation from the desired zonal temperature settings ($\hat{y}$) is much smaller with ZHT adaptation. As a result of ZHT adaptation, doors of room 3 and 4 are completely opened and the rest are closed.

ZHT adaptation also helps in scenario 2 (i.e. both zones 5 and 6 are not attached to a heat source), as shown in Figure 3a. ZHT adaptation results in complete opening of all the room doors. The total objective results represented by figure 3a shows that the benefits of ZHT adaptation is even more pronounced in this case, as compared to scenario 1. However, in this scenario, the heat energy used ZHT adaptation is more than than with no ZHT adaptation, although the difference decreases as α increases. However the corresponding temperature deviation is much better with ZHT adaptation, across the entire range of α values considered. The improvement in the temperature deviation metric $||y-\hat{y}||^2$ with ZHT adaptation more than compensates for the increase in energy cost, resulting in a lower total objective, even for small values of α. This also confirms the intuition that with less heat input sources, ZHT adaptation can be useful in getting the temperatures to be much closer to the desired values, perhaps at the expense of a small amount of additional energy.

Figure 4 shows the zonal temperature dynamics evolution under scenario 1 in which room 6 do not have a heating source. At time $t = 0$, the optimal heat inputs were applied for the initial ZHT configuration (all doors and windows closed). Then, once the zonal temperatures have all settled down to their optimal values with no ZHT adaptation, about $t = 1200$, the ZHT method was turned on and the system was allowed to reach a new steady state. It can be observed from Figure 4 that with ZHT adaptation, we are quite close to the desired temperature for zone 3 ($\sim 65^\circ F$), whereas without ZHT adaptation, this temperature is off by $5^\circ F$. At the same time, the temperature in zone 6 is much closer to the desired temperature ($\sim 67^\circ$) with ZHT adaptation. Without ZHT adaptation, we were only able to achieve $\sim 70^\circ F$ in zone 6, where the desired temperature is $65^\circ F$. While better zone temperatures are attained at the cost of increased energy (we used a small value of $\alpha = 10^{-6}$ in this case), this example demonstrates that with ZHT adaptation we may be able to attain desired zonal temperatures that are unattainable by optimizing the heat inputs alone.

The results shown so far are for a specific choice of the desired zonal temperature vector $\hat{y}$. In order to demonstrate the usefulness of ZHT adaptation in more general scenarios, we have have simulated over 1000 randomly generated $\hat{y}$ vectors. In these simulations, each element of $\hat{y}$ takes a random value between $70^\circ F$ to $80^\circ F$. For scenario 1 (only zone 6 without heat source) the mean total objective (as described in (4)) was obtained as 5.4 and 11.4, with standard deviation of 6.1 and 10.23, for the cases of with and without ZHT adaptation, respectively. For scenario 2 (zones 5 and 6 without heat source) mean total objective was obtained as 16.3 and 36.2, with standard deviation of 14.8 and 26.3, for the cases of with and without ZHT adaptation, respectively. This further demonstrates that ZHT adaptation is able to improve the objective of (4) significantly, both in terms of its mean and variance, over random choices of the preferred temperature vector $\hat{y}$.

V. Conclusion

In this paper, we explored the benefits of adapting the zonal heat transfer (ZHT) rates between the adjacent zones of a multi-zone indoor space to attain temperatures close to the desired zonal temperatures compared to no ZHT adaptation. In this work, we formulated the problem of determining the optimal ZHT configurations under steady state condition using a thermal model derived using electrical circuit analogy. While the solution of the problem requires joint determination of the optimal ZHT settings and zonal heat inputs, using closed-for expressions of the optimal heat input functions, we showed how our optimization problem can be reduced to one of determining the ZHT settings alone. We further derived a condition under which the problem is convex, and discussed additional scenarios in which the complexity/dimensionality of the model is significantly reduced. Our simulations on a realistic model of a 6-zone indoor space showed that ZHT adaptation is able to attain temperatures much closer to the desired zonal temperatures, as compared to the case of no ZHT adaptation. This is particularly the case when the number of heat (control) inputs is less than the number of thermal zones. Attaining better zonal temperatures can come at the cost of increased energy usage. Through a proper choice of the trade-off parameter α, however, it is possible to strike a good balance between thermal comfort provided to occupants in the different spatial zones, and the overall energy consumed due to heating/cooling of the space.

Acknowledgements

This work was supported by the National Science Foundation through Award No.1230687.

References

[1] T. Hilliard, *Whole building model predictive control with optimization for HVAC systems utilizing surface level weather forecasts*. PhD dissertation, Dalhousie University, 2017.

[2] D. Li, C. C. Menassa, and V. R. Kamat, "Personalized human comfort in indoor building environments under diverse conditioning modes," *Building and Environment*, vol. 126, pp. 304 – 317, 2017.

[3] T. Hilliard, L. Swan, and Z. Qin, "Experimental implementation of whole building mpc with zone based thermal comfort adjustments," *Building and Environment*, vol. 125, pp. 326 – 338, 2017.

[4] J. Borggaard, J. A. Burns, A. Surana, and L. Zietsman, "Control, estimation and optimization of energy efficient buildings," in *2009 American Control Conference*, pp. 837–841, June 2009.

[5] S. K. Gupta, K. Kar, S. Mishra, and J. T. Wen, "Building temperature control with active occupant feedback," *IFAC Proceedings Volumes*, vol. 47, no. 3, pp. 851 – 856, 2014. 19th IFAC World Congress.

[6] S. K. Gupta, K. Kar, S. Mishra, and J. Wen, "Distributed consensus algorithms for collaborative temperature control in smart buildings," *IEEE Conference on Automation Science and Engineering*, pp. 438–443, August 2016.

[7] S. K. Gupta, K. Kar, S. Mishra, and J. T. Wen, "Incentive compatible mechanism for coordinated temperature control in multi-occupant buildings," in *2015 IEEE International Conference on Automation Science and Engineering (CASE)*, pp. 438–443, Aug 2015.

[8] McBee and K. Brian, *Computational Approaches to Improving Room Heating and Cooling for Energy Efficiency in Buildings*. PhD thesis, Virginia State and Polytechnic Institute, 2011.

[9] P. Riederer, D. Marchio, J. Visier, A. Husaunndee, and R. Lahrech, "Room thermal modelling adapted to the test of HVAC control systems," *Building and Environment*, vol. 37, no. 8, pp. 777 – 790, 2002.

[10] H. Boyer, J. Chabriat, B. Grondin-Perez, C. Tourrand, and J. Brau, "Thermal building simulation and computer generation of nodal models," *Building and Environment*, vol. 31, no. 3, pp. 207 – 214, 1996.

[11] G. Fraisse, C. Viardot, O. Lafabrie, and G. Achard, "Development of a simplified and accurate building model based on electrical analogy," *Energy and Buildings*, vol. 34, no. 10, pp. 777 – 790, 2002.

[12] S. K. Gupta, S. Atkinson, I. O'Boyle, J. Drogo, K. Kar, S. Mishra, and J. T. Wen, "BEES: Real-time occupant feedback and environmental learning framework for collaborative thermal management in multi-zone, multi-occupant buildings," *Energy and Buildings*, vol. 125, pp. 142 – 152, 2016.

[13] V. L. Erickson and A. E. Cerpa, "Thermovote: Participatory sensing for efficient building HVAC conditioning," in *Proceedings of the Fourth ACM Workshop on Embedded Sensing Systems for Energy-Efficiency in Buildings*, BuildSys '12, (New York, NY, USA), pp. 9–16, ACM, 2012.

[14] L. Pérez-Lombard, J. Ortiz, and C. Pout, "A review on buildings energy consumption information," *Energy and Buildings*, vol. 40, no. 3, pp. 394 – 398, 2008.

[15] M. Minakais, S. Mishra, J. T. Wen, L. Lagace, and T. Castiglia, "Design and instrumentation of an intelligent building testbed," in *2015 IEEE International Conference on Automation Science and Engineering (CASE)*, pp. 1–6, Aug 2015.